Amato F., Perez N., Lopez M., Ripoll A., Alastuey A., Pandolfi M., Karanasiou A., Salmatonidis A., Padoan E., Frasca D., Marcoccia M., Viana M., Moreno T., Reche C., Martins V., Brines M., Minguillón M.C., Ealo M., Rivas I., van Drooge B., Benavides J., Craviotto J.M., and Querol X.

Vertical and horizontal fall-off of black carbon and NO2 within urban blocks

Science of The Total Environment Volume 686, 2019, Pages 236-245

https://doi.org/10.1016/j.scitotenv.2019.05.434

Vertical and horizontal fall-off of black carbon and NO2 within urban blocks

Amato, F.[1]*, Perez, N.[1], Lopez, M.[1], Ripoll, A.[1], Alastuey, A.[1], Pandolfi, M.[1], Karanasiou, A.[1], Salmatonidis, A.[1], Padoan, E.[1-2], Frasca, D.[3], Marcoccia, M.[3], Viana, M.[1], Moreno, T.[1], Reche, C.[1], Martins, V.[1], Brines, M.[1], Minguillón, M.C.[1], Ealo, M.[1], Rivas, I.[4], van Drooge, B.[1], Benavides J.[5], Craviotto, J.M. [6], and Querol, X.[1]

[1] *Institute of Environemntal Assessmnet and Water Research, Spanish Research Council (IDAEA-CSIC), Barcelona, Spain*

[2] *University of Turin, Turin, Italy*

[3] *Chemistry Department, Sapienza University of Rome, Rome, Italy*

[4] *ISGlobal, Barcelona, Spain*

[5] *Barcelona Supercomputing Center, Barcelona, Spain*

[6] *Barcelona City Council, Barcelona, Spain*

Keywords: decay, dispersion, road, building, vehicle emissions, diesel

*Corresponding author: fulvio.amato@idaea.csic.es

<u>Abstract</u>

While exposure to traffic pollutants significantly decrease with distance from the curb, very dense urban architectures hamper such dispersion. Moreover, the building height reduces significantly the dispersion of pollutants. We have investigated the horizontal variability of Black Carbon (BC) and the vertical variability of NO2 and BC within the urban blocks. Increasing the distance from road BC concentrations decreased following an exponential curve reaching halving distances at 25 m (median), although with a wide variability among sites. Street canyons showed sharper fall-offs than open roads or roads next to a park. Urban background concentrations were achieved at 67 m distance on average, with higher distances found for more trafficked roads. Vertical fall-off of BC was less pronounced than the horizontal one since pollutants homogenize quickly vertically after rush traffic hours. Even shallower vertical fall-offs were found for NO2. For both pollutants, background concentrations were never reached within the building height. A street canyon effect was also found exacerbating concentrations at the lowest floors of the lee-ward side of the road. These inputs can be useful for assessing population exposure, air quality policies, urban planning and for models validation.

Introduction

Urban air pollution is one of major issues for public health. The Global Burden of Disease assessment concluded that air pollution is one of the major reasons of deaths globally (GBD, 2015) mostly due to exacerbation of cardiovascular and respiratory diseases. Road traffic is often recognized as the most important source of airborne particles and NOx in large cities of Europe, and diesel exhaust emissions are also recognized as carcinogenic to humans (Group 1)(IARC, 2012). Recent findings point also at exposure to traffic related pollution as a risk factor for neurodevelopment deceleration in children (Sunyer et al., 2016). In the European Union (EU), as in many other regions of the world, a high share of population lives in areas exceeding WHO guidelines for atmospheric pollutants (EEA, 2018), based on the information recorded at the official monitoring networks. Several modelling exercises attempt then to estimate population exposure within the urban environment (Snyder et al. 2013, Berkowicz et al. 2008, Holmes and Morawska, 2006; Tiwary et al., 2009), but a large uncertainty in their modelled concentrations is due to the presence of buildings which act as barriers, road shape and orientation with respect to wind, and misrepresentation of local emissions.

Only a few experimental studies have investigated the horizontal dispersion of pollutants in urban environments in order to calibrate and/or validate modelling activities. Xing and Brimblecombe (2018) found that in roadside into urban parks at pedestrian level in Hong Kong, the downwind direction, pollutant concentrations decrease rapidly from roadside and by some tens of metres reached relatively constant values. They found an even sharper gradient in the upwind direction, with a rapid increase detected within 2 m of the road edge. Their simulations with Eulerian model suggest 17 m as a typical halving distance under normal urban conditions. Richmond-Bryant et al., (2017) found in the streets near heavy traffic road in Las Vegas (NV) that near road NO2 gradients are lower during summer compared to winter, with a steeper gradient during the summer, when convective mixing occurs during a longer portion of the day. Ducret-Stich et al. (2013) found pollutant concentrations falled-off to background levels within 150 to 200m from the highway in a rural Swiss Alpine valley crossed by the main North-south highway of Switzerland. Conversely, Wu et al. (2002) found no significant trend of decrease of PM near a major road in Macao, China. van Drooge (2013) found concentrations of benzo[a]pyrene of ~ 3 ng/m3 on the sidewalks in busy streets and ~ 0.3 ng/m3 in the urban background sites.

Roorda-Knape et al. (1998) found that black smoke and NO2 declined with distance from the roadside, but no gradient was found for PM10, PM2.5 and benzene. The gradients for NO2 and black smoke were curvilinear and more evident in periods that the city districts had been downwind from the motorway. Kodama et al. (2002) found also a tendency for outdoor NO2 concentrations to decrease with distance from the roadside, but the NO2 concentration differences between the roadside and the site far from the roadside were less than 10 ppb. Clearly, the concentrations are highest in the immediate vicinity of the road Tiitta et al. (2002) measured PM2.5 concentrations at distances of 12 and 25 m; however, the difference between the concentrations measured at the two largest distances (52 and 87 m) was not statistically significant. Considering the whole data set (including both upwind and downwind cases), traffic emissions in the road caused an increase in concentrations of approximately 30% from the nearest to the largest distances. Naser et al. (2009) found that NOx and EC concentrations at at 70 m were 26–45% and 21–55%, respectively, of the concentrations at 5 m distance from the road.

Another important lack of knowledge concerns the variation of pollutants concentration within the building height where most of people live and work. Hitchins et al. (2002) found a decrease of concentration of fine and ultra-fine particles of 50-60% from the ground level readings to full building height in Brisbane, Australia (from 24 to 33 m above the ground). Azimi et al. (2018) analyzed PMx mass and NO2 among other parameters at four floors of a skyscraper in Chicago downtown. While average PM1 and PM2.5 concentrations estimated on the top two floors were more than 30% lower than on the 2nd floor, NO2 was less consistent. Wu et al. (2002) found that at the height of 79 m, the concentrations of PM10, PM2.5 and PM1, decrease to about 60%, 62% and 80% respectively of the maximum occurring at 2 m above the ground. Kenagy et al. (2016) investigated the variability in the first 2 m at several UK roads, finding that at 0.8 m measured concentrations were 5–15 % greater than at 2.0 m, but such difference was not observable at distances 2.5 m or greater from the kerbside. Chan et al. (2000) found that in street canyons in the urban area of Hong Kong, TSP and PM10 concentration varies exponentially with height, where the PM dispersion is affected by the prevailing wind direction and the street configuration, in particular the height-to-width (aspect ratio). Detailed information is needed in order to avoid a misrepresentation of pollutant's spatial variation. A correct interpretation of the spatial variation of pollutants influences the quality of urban infrastructures such as a bicycle lanes, kindergartens, schools, daycare centres and hospitals, with the objective of reducing population exposure. In this study we present novel results on the vertical and horizontal variability of diesel-related pollutants (NO_2 and BC) within urban blocks of Barcelona, Spain, considering several road geometries in relation also to wind patterns, with the main goal of providing experimental evidence for modelling validation.

The objectives of the study were the following: i) describing the dispersion of BC away from road (horizontally and vertically); ii) describing the vertical dispersion of NO2 away from road; iii) identifying the main factors controlling dispersions; iv) identifying the mean distances, at which pre-defined reduction thresholds are reached. Our results offer insights for improving exposure studies and for urban planning.

2. Methods

2.1. Study area

The city of Barcelona lies along the western coast of the Spanish Mediterranean Basin, and it is delimited by two river basins (Besòs in the North and Llobregat in the South) and the Catalan coastal range in the West. The city is densely populated (15.880 inhabitants/km^2) counting 1.6 million inhabitants which become double when the metropolitan area is concerned (36 municipalities).

While the public transportation inside the city is well developed, 25% of travels are performed by private vehicles, with a significant contribution from/to the metropolitan area (25% of travels, half of them by private vehicles) and an aged freight distribution fleet (Ajuntament de Barcelona, 2016). Diesel engines are still an important share of circulating vehicles in the Province of Barcelona: 51% of passenger cars and 87% of duty vehicles (DGT, 2016). Consequently, the city suffers poor air quality in terms of particulate matter and NO2 mostly due to road traffic emissions, although other significant contributions to PM levels are originated from industries, harbour and urban works (Amato et al., 2016). Moreover the low wind speed and dense urban architecture, characterized by street canyons, hampers the dispersion of traffic pollutants, provoking accumulation of pollutants where people live and work.

2.2. Measurements

Air quality monitoring included:

- $NO2$ by means of diffusion tubes (Gradko) which collect passively during 2-3 weeks NO2 molecules and absorb them into a triethanolamine impregnated filter which is analysed by ion chromatography after sampling to determine $NO2^-$ concentrations which are then corrected into NO2 concentrations averaged along the exposure period.
- black carbon (BC) by means of AE-51 micro-aethalometers (Aethlabs) with a time resolution of 30 seconds.

Three different campaigns were carried out:

- 29 horizontal profiles of BC, from the road edge until a maximum distance of 250 m. The distance between the 8 monitors was varying from site to site, depending on local conditions. The 8 monitors were simultaneously deployed for the measurements along a given transect. Measurements were undertaken during 30 minutes in four different days, between 9 AM and 6 PM. In order to minimize the interference of surrounding roads, BC monitors were located along pedestrian areas or very low intensity traffic roads.
- 28 vertical profiles for NO_2. At 18 buildings at least 1 diffusion tube was installed outdoor at each floor, including ground floor and the roof during a period of 2-4 weeks, Figure 1. At several buildings profiles were repeated, so that 28 profiles were obtained. The raw concentrations were corrected after inter-comparison with chemi-luminescence reference instrumentation at 5 monitoring stations in the city. Precision was evaluated by means of collocation of duplicates.
- 4 vertical profiles of BC starting from 2.5-6 m height. At 4 buildings BC monitors were installed outdoor at each floor, including ground floor and the roof during a period varying from 4 hours to 3 days, Figure 1. The raw concentrations were corrected after inter-comparison among the different monitors, using the mean value as reference value for correction.

Data were used both in absolute concentrations (ng/m^3 for BC and µg/m^3 for NO2) and normalized concentrations, dividing each value by the initial one (road edge for horizontal profile) and lowest floor for vertical profiles).

The following additional data were collected during the measurements:

- Wind data were obtained at the roof of the University of Barcelona (Faculty of Physics, (41º 23' 04, 59'' N; 2º 07' 04, 99'' E). For horizontal profiles, we calculated the wind component (WS_{st}) in the direction parallel to the vector emitting road-receptors as:

$$WS_{st} = cos(WDca - \alpha)\ WSca$$

Where $WDca$ and $WSca$ are wind direction and speed at the canopy level and α is the angle between the North and such vector.

- BC and NO2 concentrations measured at the urban underground Palau Reial monitoring station (41º 23’ 14,20’’ N; 2º 06’ 56,39’’ E)
- NO2 concentration measured at the Eixample traffic monitoring station from local network (41º 23’ 07,33’’ N; 2º 09’ 14,53’’ E).
- Planetary boundary layer (PBL) height as measured by radio soundings performed at the University of Barcelona, Faculty of Physics.

3. Results and Discussion

3.1. QC/QA

Eleven NO2 diffusion tubes were intercompared, during summer and winter 2016, with chemi-luminescence reference method obtaining a correction factor of 0.83 (R2= 0.82). Twelve duplicate tubes delivered a mean deviation of <2% from each other. The eight black carbon instruments were inter-compared several times during the measurement campaign providing all a Pearson correlation coefficient ≥ 0.8 (p<0.01). For BC correction the mean value was used as reference but only instruments delivering a deviation from the mean < 20% were considered for the mean.

3.2. Horizontal profiles of BC

In Total 29 BC horizontal profiles were obtained (Table 1) and grouped within four main categories according to the urban architecture:

- street canyons (district of *Eixample*) with approximately 20 m wide one-way roads and 20(-30 m) height continuous building blocks. Three roads with aspect ratios within 0.9-1.3 were characterized.
- old district/deep canyon (*Travessera de Gràcia*) with 4 m wide one-way roads and 16 m height buildings. Aspect ratio 4.3
- open road (Diagonal Avenue), with 80 m wide two-ways urban roads and quite variable building height.
- urban park (Paseo Picasso), a 20 m wide road delimited by 20 m buildings on one side and a park on the other side.
- two ring roads: two-ways roads with six-lanes (plus four additional ones for one ring road) with sporadic buildings.

Thirty-minutes averaged BC concentrations at the road edge varied within 3.5 and 19.8 µg/m^3, being 2-16 times higher than the simultaneous background concentration measured at the Palau Reial station. Such high variation is due to multiple factors such as traffic conditions (intensity and congestion), road aspect ratio and orientation and wind conditions, in fact the highest ratios (>9) with respect to the background levels were recorded regardless of road categories. When increasing the distance from road edge BC concentrations were reduced, being data points quite well fitted by an exponential curve (R^2 within 0.18 and 0.92, Figure 2). According to the least squares fit, halving distances were reached already at 25 m (median), although with a quite wide deviation (total standard deviation of 35 m), even for the same road. Even if the different road categories do not show clearly different decreasing curves (Figure 3), it is possible to observe a tendency towards higher exponents (sharper fall-offs) for the old district deep canyon and street canyons, and lower exponents (smoother fall-offs) for the urban park. The ring roads showed a clear separation according to wind scenario (sharper fall-offs measured downwind (i.e. with positive WS_{st}). The profiles obtained at the open road (Diagonal Avenue) span over the entire distribution (Figure 3 and Table 1) in spite of belonging all to one road only H1, H2 and H5 profiles showed sharper fall-offs since they were measured in fully pedestrian areas, while H3, H4, H11, H16 and H23 were measured along the sidewalk of a (very) quiet road (with no exit) but still with sporadic vehicles. Since there was no significant difference in traffic intensity or in wind speed among the two groups of profiles in Diagonal Avenue, this result suggests that pedestrian areas show larger fall-offs than areas with restricted traffic (only for residents or goods transportation for example). Concentrations measured at halving distances were however systematically above the urban background concentration measured at Palau Reial (0.8-7.3 µg/m3), which were reached at much higher distances (67m, as median of 8-285 m range) according to the exponential regression curves. Table 2 summarizes the mean halving distances and the distance where background concentrations were achieved for the five road categories. We found that the higher the traffic intensity of the road category, the higher is the distance where background concentrations were reached (R^2=0.49). This suggests that the impact of the closest road segment is dominating that of surrounding roads (e.g. 1 km^2), at least under no atmospheric stagnation, even in a dense road structure such as the city of Barcelona, where blocks are all separated by intense roadways, at least in periods with no calm.

3.3. Vertical profiles

Totally 28 NO2 and 4 BC vertical profiles were obtained (Table 3) and grouped within the four aforementioned road categories. The NO2 vertical profiles only offer one mean concentration at each height, while the BC data are available with a 5-minutes time resolution at each height. NO2 concentrations at ground floor (<4 m height) were registering concentrations within 31-66 µg/m^3 (47 µg/m^3 as mean) while the traffic monitoring station "Eixample" was measuring 46-65 µg/m^3 (50 µg/m^3 as mean), revealing a good representativeness of that traffic station (Figure 4). NO2 concentrations were reduced moving upward over the façade, being quite well simulated by a least squares regression with an exponential curve (R2 within 0.08-0.91). According to the best regression curves (R^2 >0.6, 11 profiles), half concentrations (with respect to ground concentrations) were almost never reached within building height, but well above the roof level (25-99 m), although such values could be overestimated due to the greater dispersion above roof level. Only 10% reduction was achieved within 3 and 15 m (first to fifth floor approximately). This highlights the low dispersion of NO2 within blocks height, even at relatively open roads. In fact no significant differences in dispersion patterns were observed among different road categories (i.e. aspect ratios).

Background concentrations as measured at the Palau Reial monitoring station would be achieved at 39 m on average (only R^2 >0.6) (well above the typical roof level in Barcelona, Fig. S1 but with a large variability, varying within 4 and 107 m. At street canyons background concentrations were reached at height about twice with respect old district/deep canyon road.

Four of the 28 vertical profiles of NO2, were also characterized for BC. These buildings were located at 1 open road, 2 street canyons and 1 deep canyon in the old district. BC regression curves delivered again quite good fit (R2 within 0.39-0.77). The mean dilution pattern of BC can be described as an exponential reduction implying a halving height (with respect to ground concentration) at 26-46 m, which is about half the NO2 halving height. In all four cases BC vertical dilution was therefore greater than for NO2 due to the solid phase of BC and probably also to the partially secondary primary origin of NO2 (Figure 5). Ten percent BC reduction was obtained at 4-7 m height. Therefore BC falled-off much less in the vertical direction than in the horizontal one, indicating that upward transport of traffic related particles is probably more efficient than the horizontal one.

BC measurements allowed also exploring possible changes of intra-daily vertical distribution. In the V32 profile (open road, Figure 6a) we observed four peaks in morning hours (coinciding at all heights) separated approximately 30 min each other (from 09:00 to 11:00) with a rather constant concentration within the first 22 m and a quick dilution just above roof level. Top/bottom ratio was around 0.3-0.4 but reaching quickly an homogenization towards a ratio of 0.8 related likely to the upwards movement of BC particles due to surface warming. This smoother fall-off curve remained stable until the end of measurement (16:00). A similar pattern was observed at V30 profile (street canyon, Figure 6b) even if the roof level was 5 m lower, indicating a clear dilution over the façade, regardless of the building height. From 11:30, the same mixing observed in V32 was found at V30, even when concentrations rose at 12:00. At another street canyon (V31 profile, Figure 6c) the morning peak hour registered an important dilution already at the second floor (9.5 m). The differences between V30 and V31 are the higher traffic intensity at V30 and the road orientation (V30 is oriented SE-NW, while V31 is perpendicular).

Afternoon and night measurements were performed only at V29 profile, a street canyon oriented parallel to sea breeze. At this site the same pattern observed at V31 and V32 was found, both in morning and afternoon peak hours, while in the night the concentrations were very similar at all heights, including the roof level (Figure 6d).

Several studies have modelled 3D spatial distribution of air pollutants within street canyons, identifying a lee-ward (upwind with respect to main wind direction) side accumulation of pollutants, the so-called "street canyon effect", with respect to the wind-ward side (Berkowicz, 2000). In order to validate this hypothesis with our experimental data, we compared the exponents of fall-off curves of NO2 on roads perpendicular (SE-NW) to the main wind direction (sea breeze) separating two groups: i) those obtained at buildings on the lee-ward side and ii) on the windward side. We also compared the two sides of the roads in the perpendicular direction (parallel to wind), where no "street canyon effect" is expected. Results show a significant difference in the exponent values obtained at buildings on the lee-ward (higher exponent) and windward (lower exponent, Figure 7). This result indicates that at the leeward side NO2 profiles are less homogeneous tan at the windward side, i.e. the difference between lower floors and higher floor is higher than at the windward side. Such statistically significant difference was not observable instead in the roads parallel to the main wind direction (Figure 7).

Conclusions

Reduction of BC concentration with increasing distance from road edge followed nicely an exponential curve. Halving distances were reached already at 25 m (median), although with a quite wide deviation (total standard deviation of 35 m), even for the different periods for the same road. However, a trend towards higher exponents (sharper fall-offs) for the old district/deep canyon (low traffic density, very narrow streets) and street canyons, and lower exponents (smoother fall-offs) for the urban park, was observed. Open roads (including ring roads) were more affected by wind conditions (sharper fall-offs measured downwind). Concentrations measured at halving distances were however systematically above the urban background concentrations which were achieved at 67m (8-285 m range), indicating the difficulty to reach background conditions within the city center. We found that the higher the traffic intensity of the road category, the higher the distance where background concentrations are reached, suggesting that the impact of the closest road segment is dominating that of surrounding roads (e.g. 1 km^2), at least under no atmospheric stagnation.

Vertical fall-off of BC was less pronounced than the horizontal one, with a halving height (with respect to ground concentration) at 26-46 m, indicating that particle transport is mostly upwards and that concentrations homogenize quickly after rush traffic hours (when vertical fall-off is sharper). During night no significant variability was observed within building height. Even smaller vertical fall-offs were found for NO2 (twice the halving height of BC), due to its gaseous phase and partially secondary origin. For both pollutants, background concentrations were never reached within the building height. A significant difference in fall-off rate was found between different sides of street canyons: although these data are limited by the fact that we compared buildings in different roads, the high number of sites allowed us to conclude that sharper fall-offs occur at the leeward side, due to pollutants accumulation in the lowest floor.

Acknowledgments

Funding from the City Council of Barcelona is acknowledged (Contract: "*Estudio sobre la variación de los niveles de concentración de contaminantes atmosféricos en función de la altura 15002577*"). Authors are also thankful to the University of Barcelona (Department of Physics) and ISGlobal for instrumental support. Funding from the City Council of Barcelona by the Generalitat de Catalunya (AGAUR 2017 SGR41) is acknowledged.

Bibliography

Amato, F., Alastuey, A., Karanasiou, A., Lucarelli, F., Nava, S., Calzolai, G., Severi, M., Becagli, S., Gianelle, V.L., Colombi, C., Alves, C., Custódio, D., Nunes, T., Cerqueira, M., Pio, C., Eleftheriadis, K., Diapouli, E., Reche, C., Minguillón, M.C., Manousakas, M.-I., Maggos, T., Vratolis, S., Harrison, R.M., Querol, X. AIRUSE-LIFE+: A harmonized

PM speciation and source apportionment in five southern European cities (2016) Atmospheric Chemistry and Physics, 16 (5), pp. 3289-3309.

Azimi, P., Zhao, H., Fazli, T., Zhao, D., Faramarzi, A., Leung, L., Stephens, B. Pilot study of the vertical variations in outdoor pollutant concentrations and environmental conditions along the height of a tall building (2018) Building and Environment, 138, pp. 124-134.

Berkowicz (2000), OSPM - A Parameterised Street Pollution Model. Environmental Monitoring and Assessment 65: 323–331, 2000.

Berkowicz, R., Ketzel, M., Jensen, S.S., Hvidberg, M., Raaschou-Nielsen, O. Evaluation and application of OSPM for traffic pollution assessment for a large number of street locations (2008) Environmental Modelling and Software, 23 (3), pp. 296-303.

Chan, L.Y., Kwok, W.S. Vertical dispersion of suspended particulates in urban area of Hong Kong (2000) Atmospheric Environment, 34 (26), pp. 4403-4412.

Ducret-Stich, R.E., Tsai, M.-Y., Ragettli, M.S., Ineichen, A., Kuenzli, N., Phuleria, H.C. Role of highway traffic on spatial and temporal distributions of air pollutants in a Swiss Alpine valley

(2013) Science of the Total Environment, 456-457, pp. 50-60

EEA (2018) Air quality in Europe - 2018 report. EEA (European Environment Agency) Published: 29 Oct 2018. ISBN: 978-92-9213-990-2.

Holmes, N.S., Morawska, L. A review of dispersion modelling and its application to the dispersion of particles: An overview of different dispersion models available (2006) Atmospheric Environment, 40 (30), pp. 5902-5928.

GBD 2013 Risk Factors Collaborators, Forouzanfar, M. H., Alexander, L., Anderson, H. R., Bachman, V. F., Biryukov, S., et al. (2015). Global, regional, and national comparative risk assessment of 79 behavioural, environmental and occupational, and metabolic risks or clusters of risks in 188 countries, 1990e2013: A systematic analysis for the global burden of disease study 2013. Lancet (London, England), 386(10010), 2287e2323. http://dx.doi.org/10.1016/S0140-6736(15)00128-2

Hitchins, J., Morawska, L., Gilbert, D., Jamriska, M. Dispersion of particles from vehicle emissions around high- and low-rise buildings (2002) Indoor Air, 12 (1), pp. 64-71.

Kenagy, H.S., Lin, C., Wu, H. et al. Greater nitrogen dioxide concentrations at child versus adult breathing heights close to urban main road kerbside. Air Qual Atmos Health (2016) 9: 589. https://doi.org/10.1007/s11869-015-0370-3

Kodama, Y., Arashidani, K., Tokui, N., Kawamoto, T., Matsuno, K., Kunugita, N., Minakawa, N., 2002. Environmental NO2 concentration and exposure in daily life along main roads in Tokyo. Environmental Research 89, 236–244.

IARC, 2012. DIESEL ENGINE EXHAUST CARCINOGENIC. PRESS RELEASE N° 213 12 June 2012. https://www.iarc.fr/en/media-centre/pr/2012/pdfs/pr213_E.pdf

Minakawa, N., Takahashi, K., Nagamune, Y., Sasaki, J., 2000a. Quality assurance of samplers for suspended particulate matter and their application to field analysis. Bunseki Kagaku 49, 619–624.

Naser, T.M., Kanda, I., Ohara, T., Sakamoto, K., Kobayashi, S., Nitta, H., Nataami, T. Analysis of traffic-related NOx and EC concentrations at various distances from major roads in Japan

(2009) Atmospheric Environment, 43 (15), pp. 2379-2390.

Richmond-Bryant, J., Chris Owen, R., Graham, S., Snyder, M., McDow, S., Oakes, M., Kimbrough, S. Estimation of on-road NO2 concentrations, NO2 /NOX ratios, and related roadway gradients from near-road monitoring data (2017) Air Quality, Atmosphere and Health, 10 (5), pp. 611-625.

Roorda-Knape, M.C., Janssen, N.A.H., De Hartog, J.J., Van Vliet, P.H.N., Harssema, H.,Brunekreef, B., 1998. Air pollution from traffic in city districts near major motorways. Atmospheric Environment 32, 1921–1930.

Snyder, M.G., Venkatram, A., Heist, D.K., Perry, S.G., Petersen, W.B., Isakov, V. RLINE: A line source dispersion model for near-surface releases (2013) Atmospheric Environment, 77, pp. 748-756

Sunyer, J., Esnaola, M., Alvarez-Pedrerol, M., Forns, J., Rivas, I., López-Vicente, M., Suades-González, E., Foraster, M., Garcia-Esteban, R., Basagaña, X., Viana, M., Cirach, M., Moreno, T., Alastuey, A.é., Sebastian-Galles, N.ú., Nieuwenhuijsen, M., Querol, X. Association between Traffic-Related Air Pollution in Schools and Cognitive Development in Primary School Children: A Prospective Cohort Study (2015) PLoS Medicine, 12 (3), art. no. e1001792, 24 p.

Tiitta, P., Raunemaa, T., Tissari, J., Yli-Tuomi, T., Leskinen, A., Kukkonen, J., Härkönen, J., Karppinen, A. Measurements and modelling of PM<inf>2.5</inf> concentrations near a major road in Kuopio, Finland (2002) Atmospheric Environment, 36 (25), pp. 4057-4068

Tiwary, A., Sinnett, D., Peachey, C., Chalabi, Z., Vardoulakis, S., Fletcher, T., Leonardi, G., Grundy, C., Azapagic, A., Hutchings, T.R. An integrated tool to assess the role of new planting in PM<inf>10</inf>capture and the human health benefits: A case study in London (2009) Environmental Pollution, 157 (10), pp. 2645-2653.

van Drooge B.L. (2013). Human Exposure to Polycyclic Aromatic Hydrocarbons in Urban and Rural Ambient Air. In: L.L. McConnell, J. Dachs, C.J. Hapeman (Ed.). Occurrence, Fate and Impact of Atmospheric Pollutants, ACS Books. Chapter 4, pp 59-82.

Xing, Y., Brimblecombe, P. Dispersion of traffic derived air pollutants into urban parks (2018) Science of the Total Environment, 622-623, pp. 576-583.

Wu, Y., Hao, J., Fu, L., Wang, Z., Tang, U. Vertical and horizontal profiles of airborne particulate matter near major roads in Macao, China (2002) Atmospheric Environment, 36 (31), pp. 4907-4918.

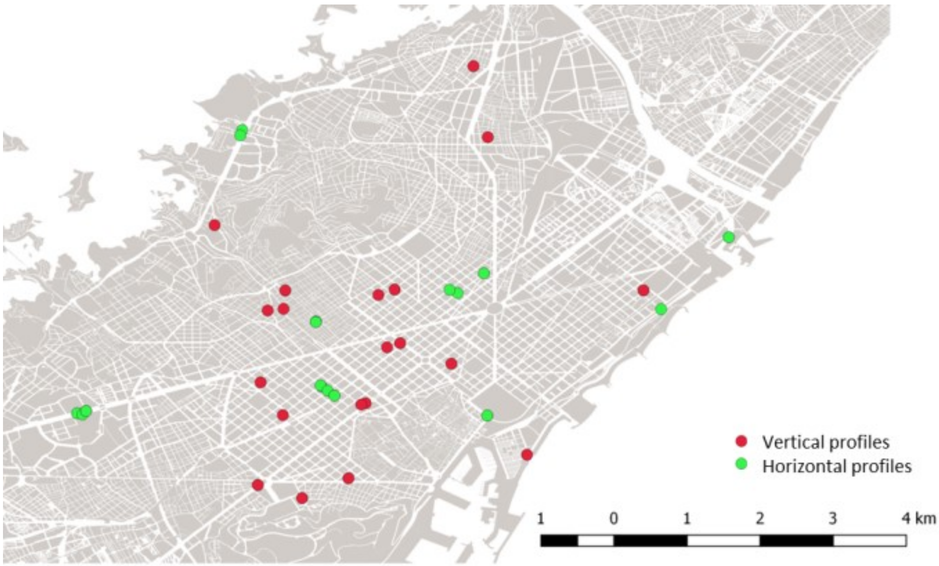

Figure 1. Map of the locations of the BC horizontal profiles and NO2 and BC vertical profiles. At most locations, duplicated profiles were obtained.

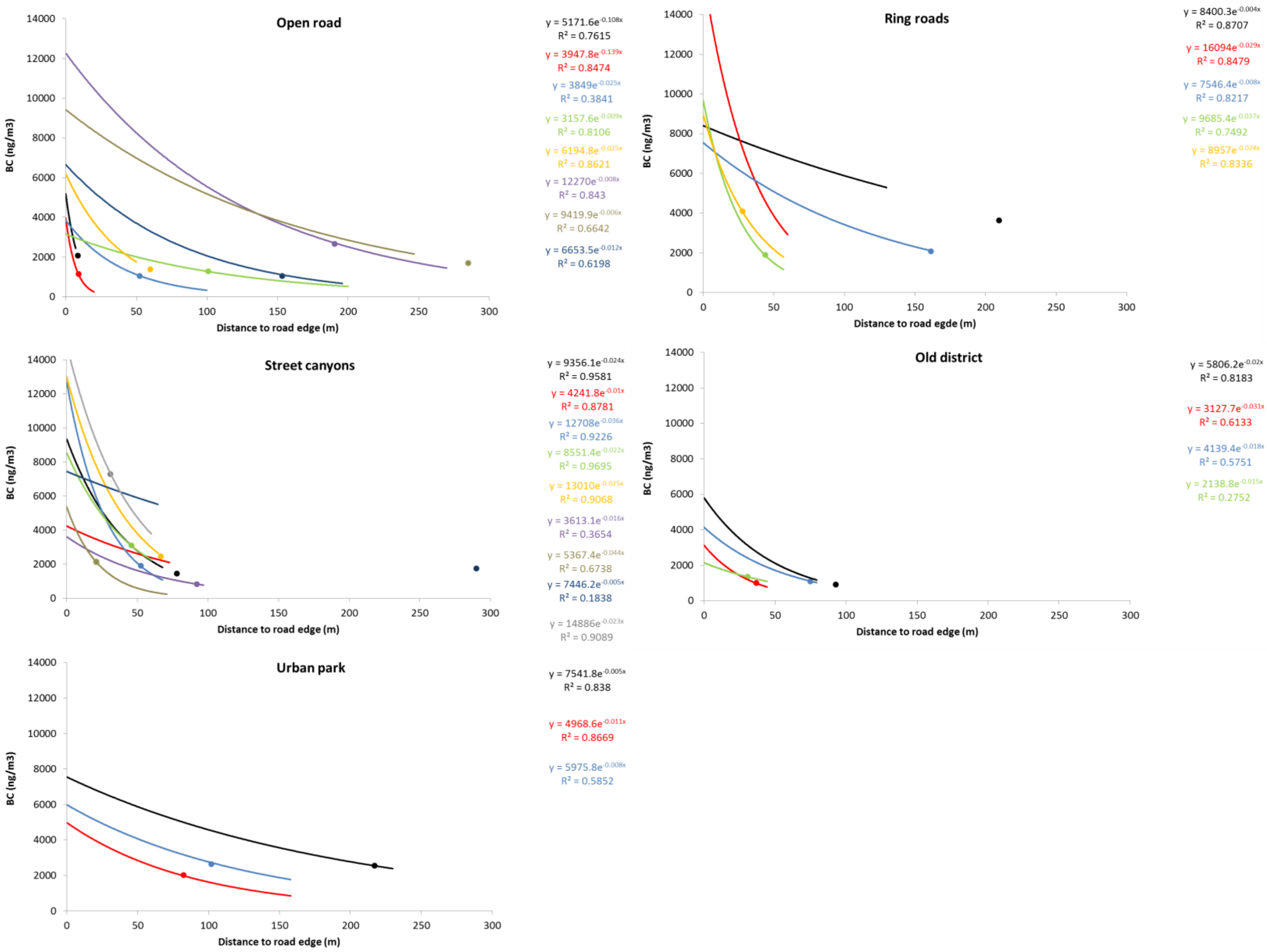

Figure 2. Regression curves for BC horizontal profiles separated per road category. Points represent the simultaneous background concentrations obtained at the Palau Reial monitoring site in the same periode

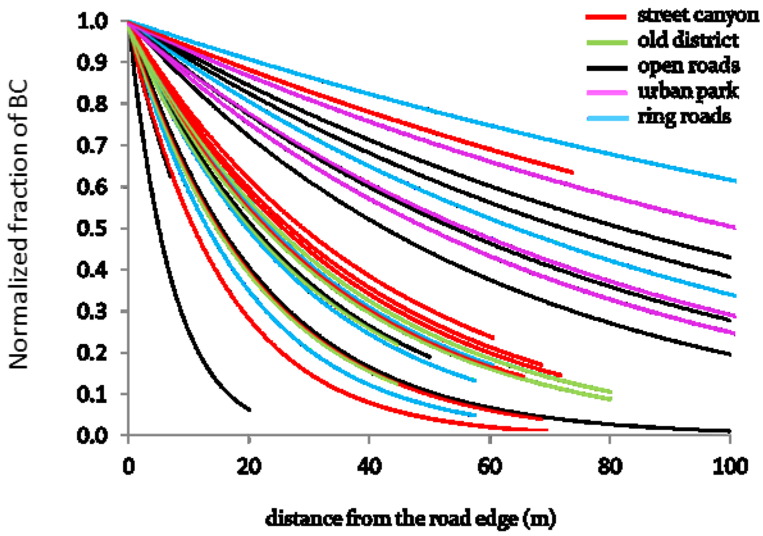

Figure 3. Normalized regression curves for BC horizontal profiles separated per road category.

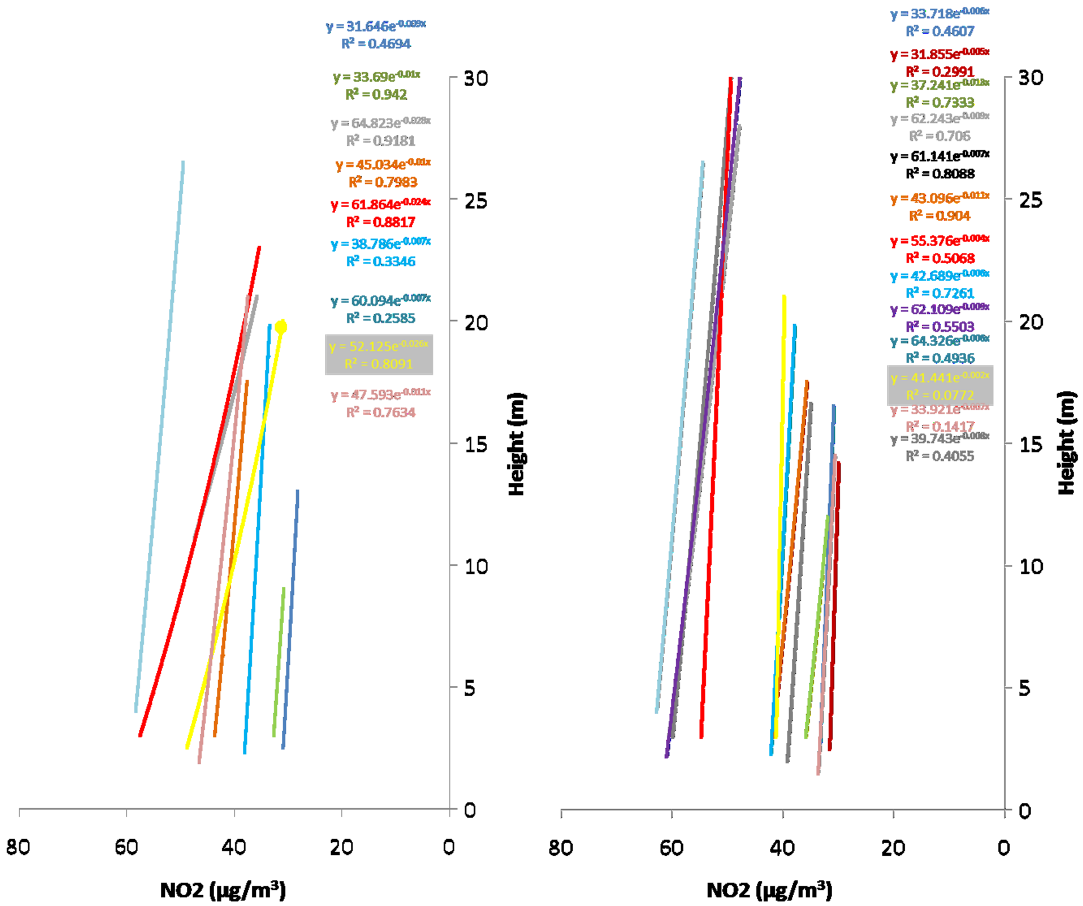

Figure 4. Regression curves for NO2 vertical profiles separated in two campaigns (one plot each) to improve readability.

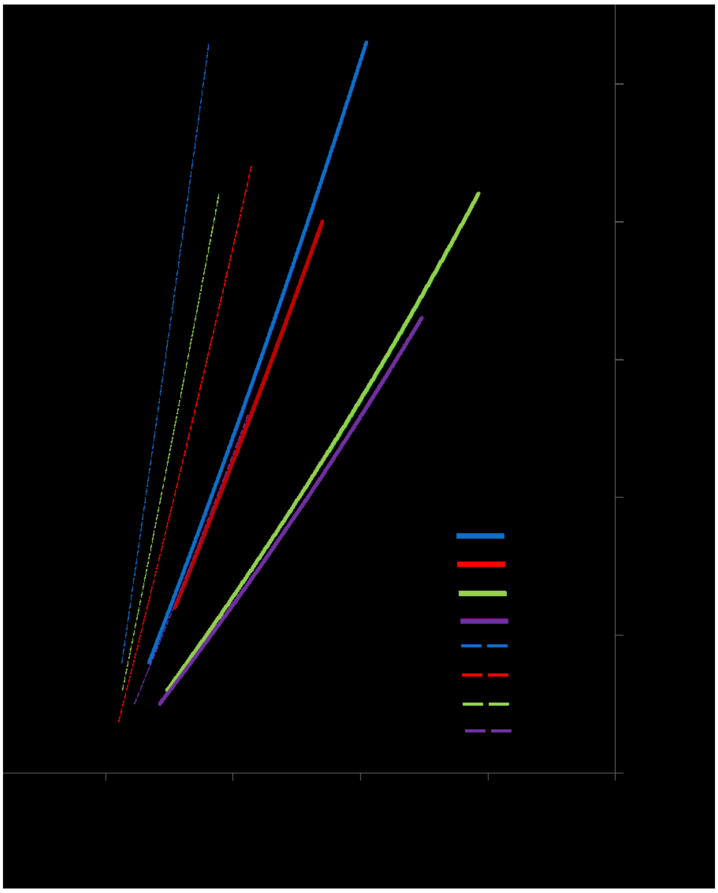

Figure 5. Comparison of vertical fall-off curve for NO2 (dotted lines) and BC (solid lines) at four buildings. Values are normalized versus the lowest height concentration.

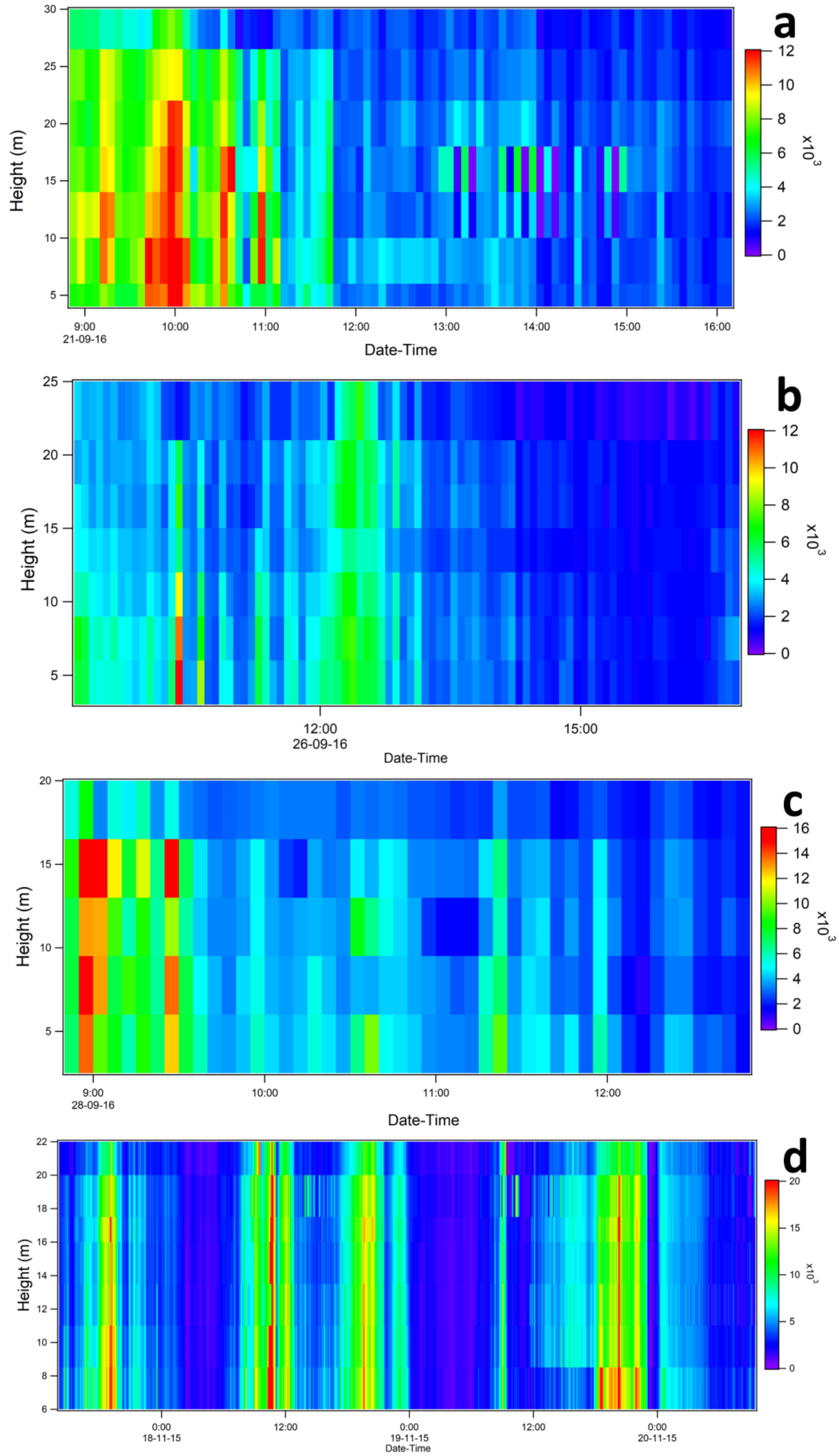

Figure 6. Time variability of BC vertical profile (ng/m^3) at four buildings (a:V32;b:V30;c:V31;d:V29).

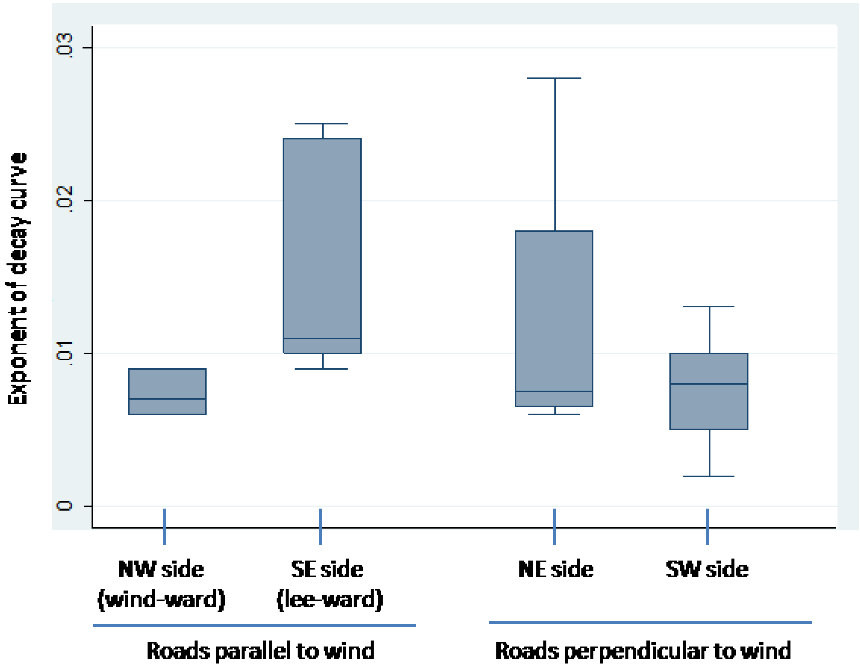

Figure 7. Variability of exponent of fall-off curve depending on road direction and side of the road.

Code	**Target road**	**Long**	**Lat**	**Width** m	**Height** m	***Aspect ratio***	**Traffic intensity** veh/day	**Day**	**Start time**	**End time**	**Wind speed** m/s	**Wind direction** °	**WSst** m/s	**PBL** m	**BC background** ng/m^3	**NO_2 background** $\mu g/m^3$	**NO_2 traffic** $\mu g/m^3$
H1	**Diagonal**	2.118558	41.386211	81.6	8.5	0.1	109600	14/01/15	9:04	9:25	1.7	234	0.3	589	1391	30	72
H2	**Diagonal**	2.118558	41.386211	81.6	8.5	0.1	109600	14/01/15	9:35	9:50	2.1	24	-1.4	589	1137	23	54
H3	**Diagonal**	2.119997	41.386582	81.6	8.5	0.1	109600	14/01/15	11:45	12:01	2.2	308	-2.0	589	1043	13	68
H4	**Diagonal**	2.119997	41.386582	81.6	8.5	0.1	109600	14/01/15	12:06	12:22	1.4	319	-1.3	589	1275	16	68
H5	**Diagonal**	2.119422	41.386017	81.6	8.5	0.1	109600	14/01/15	12:31	12:46	1.4	217	-1.3	589	2080	39	77
H6	**Mallorca**	2.158522	41.390649	18.6	24.5	1.3	26600	14/01/15	15:50	16:04	1.0	225	0.0	589	1442	31	86
H7	**Mallorca**	2.15838	41.390773	18.6	24.5	1.3	26600	14/01/15	16:16	16:26	0.8	215	0.1	589	na	27	86
H8	**Valencia**	2.159547	41.389897	17.6	23.5	1.3	23100	14/01/15	16:33	16:43	0.7	201	0.3	589	1912	44	95
H9	**Valencia**	2.180803	41.405883	17.6	19.0	1.1	31400	14/01/15	17:41	17:51	0.5	176	0.2	589	3109	61	94
H10	**Mallorca**	2.179494	41.406431	18.6	17.5	0.9	28000	14/01/15	17:57	18:07	0.7	151	0.6	589	2461	61	94
H11	**Diagonal**	2.119997	41.386582	81.6	8.5	0.1	109600	15/01/15	10:22	10:32	1.4	240	0.2	389	2673	62	67
H12	**Ronda Dalt**	2.145576	41.432575	31.9	-	-	167000	15/01/15	11:24	11:39	1.8	243	-1.2	389	3630	63	67
H13	**Ronda Dalt**	2.145251	41.431717	31.9	-	-	167000	15/01/15	12:05	12:19	1.9	239	-1.1	389	na	48	na
H14	**Ronda Litoral**	2.21411	41.40324	75.0	-	-	119300	15/01/15	15:00	15:15	2.1	234	0.5	389	2077	37	49
H15	**Pg Picasso**	2.185667	41.385836	50.9	17.0	0.3	12400	15/01/15	16:13	16:28	1.6	231	1.6	389	2545	65	57
H16	**Diagonal**	2.119997	41.386582	81.6	8.5	0.1	109600	03/11/15	9:45	10:10	2.0	228	0.6	850	1704	25	59
H17	**Trav. Gracia**	2.157625	41.401218	3.7	16.0	4.3	11200	03/11/15	11:10	11:35	2.0	244	-0.5	850	906	16	58
H18	**Trav. Gracia**	2.157605	41.401155	3.7	16.0	4.3	11200	03/11/15	11:41	12:15	2.0	245	0.5	850	1001	15	54
H19	**Valencia**	2.185116	41.409121	17.6	15.0	0.9	31400	03/11/15	13:02	13:35	2.0	238	-0.4	850	828	12	46
H20	**Arago**	2.160658	41.389114	28.2	24.5	0.9	79700	03/11/15	18:45	19:10	1.0	162	0.9	850	2141	49	100
H21	**Ronda Litoral**	2.225174	41.415029	75.0	-	-	119300	03/11/15	17:21	17:56	0.6	235	0.4	850	1897	31	86
H22	**Pg Picasso**	2.185667	41.385836	50.9	17.0	0.3	12400	03/11/15	16:14	16:49	1.3	239	1.3	850	2011	17	57
H23	**Diagonal**	2.119997	41.386582	81.6	8.5	0.1	109600	09/11/15	9:25	10:01	1.6	271	-0.7	723	1056	16	44
H24	**Trav. Gracia**	2.157625	41.401218	3.7	16.0	4.3	11200	09/11/15	10:51	11:27	2.2	276	-1.6	723	1078	17	38
H25	**Trav. Gracia**	2.157605	41.401155	3.7	16.0	4.3	11200	09/11/15	11:32	12:12	2.5	264	1.4	723	1348	16	33
H26	**Valencia**	2.185116	41.409121	17.6	15.0	0.9	31400	09/11/15	12:51	13:25	2.3	270	-1.6	723	1747	29	45
H27	**Arago**	2.160658	41.389114	28.2	24.5	0.9	79700	09/11/15	17:06	17:42	1.0	134	1.0	723	7288	43	97
H28	**Ronda Litoral**	2.225174	41.415029	75.0	-	-	119300	09/11/15	15:56	16:33	0.5	180	-0.3	723	4084	27	73
H29	**Pg Picasso**	2.185667	41.385836	50.9	17.0	0.3	12400	09/11/15	14:51	15:27	1.4	238	0.3	723	2644	21	61

Table 1. List of BC horizontal profiles and additional relevant parameters. na: not available

Table 2. Summary of statistics for horizontal BC profiles

Road category	Mean ratio above background	Median Halving distance(m)	Mean distance to achieve background (m)	Traffic intensity (veh/day)
Old district/deep canyon	6.5±3.7	22	56	11.200
Street canyons	6.9±4.4	26	49	20.000-80.000
Urban park	3.7±0.3	58	102	12.400
Open road	6.3±3.3	32	80	109. 600
Ring roads	5.0±3.1	23	103	120.000-170.000

Code	Longitude	Latitude	Adress	Start date	End date	NO_2 background µg/m³	NO_2 traffic µg/m³	BC background ng/m³	Precipitation mm	Canopy wind speed m/s	Building height m	Traffic intensity
						NO_2						
V1	2.21122	41.40634	Ramon Turró 337	07/06/16	01/07/16	27.0	49.0	1159	14.6	1.8	16.5	2878
V2	2.18340	41.44304	Tissó 32	08/06/16	01/07/16	26.3	48.3	1122	14.6	1.8	12	2309
V3	2.19216	41.37942	Pg. Marítim 5	07/06/16	01/07/16	27.0	49.0	1159	14.6	1.8	12	10014
V4	2.15233	41.40330	Gran de Gracia 190	13/06/16	11/07/16	28.1	49.1	1215	14.6	1.8	21	9398
V5	2.16784	41.40558	Sicilia 321	08/06/16	01/07/16	26.3	48.3	1122	14.6	1.8	9.5	7650
V6	2.17979	41.39432	Ausias Marc 78	20/06/16	11/07/16	31.1	52.3	1364	0.4	1.6	17.5	11843
V7	2.17050	41.40647	Industria 90	20/06/16	11/07/16	31.1	52.3	1364	0.4	1.6	15	14162
V8	2.15221	41.38591	Mallorca 106	09/06/16	11/07/16	28.0	49.2	1188	14.6	1.8	23	20640
V9	2.16294	41.37558	Viladomat 2	10/06/16	11/07/16	27.7	48.8	1184	14.6	1.8	19.8	6205
V10	2.17140	41.39769	Pg. Sant joan 75	13/06/16	01/07/16	25.7	47.3	1073	14.6	1.9	32.2	15769
V11	2.14812	41.37446	Plaza España 2	20/06/16	11/07/16	31.1	52.3	1364	0.4	1.6	26.5	117052
V12	2.15536	41.37232	Lleida 38	22/06/16	11/07/16	31.2	51.7	1326	0.4	1.6	20	8603
V13	2.15536	41.37232	Torrent de l'Olla 218	17/11/15	01/12/15	45.3	65.4	2092	0.0	2.4	21	9916
V14	2.14104	41.41701	Vallcarca 205	08/09/16	26/09/16	28.1	45.9	1128	41.6	1.8	14.5	12352
V15	2.14973	41.40304	Princep d'Asturies 23	08/09/16	26/09/16	28.1	45.9	1128	41.6	1.8	16.6	102667
V16	2.17140	41.39769	Pg. Sant Joan 75	08/09/16	26/09/16	28.1	45.9	1128	41.6	1.8	32.2	15769
V17	2.17979	41.39432	Ausias Marc 78	08/09/16	26/09/16	28.1	45.9	1128	41.6	1.8	17.5	11843
V18	2.14857	41.39126	Villaroel 237	08/09/16	26/09/16	28.1	45.9	1128	41.6	1.8	21	13314
V19	2.16294	41.37558	Viladomat 2	08/09/16	26/09/16	28.1	45.9	1128	41.6	1.8	19.8	6205
V20	2.21122	41.40634	Ramon Turró 337	13/09/16	28/09/16	29.0	50.2	1141	32.8	1.9	16.5	2878
V21	2.18575	41.43141	Irlanda 15	13/09/16	28/09/16	29.0	50.2	1141	32.8	1.9	14.2	3041
V22	2.18340	41.44304	Tissó 32	13/09/16	28/09/16	29.0	50.2	1141	32.8	1.9	12	2309
V23	2.17050	41.40647	Industria 90	13/09/16	28/09/16	29.0	50.2	1141	32.8	1.9	15	14162
V24	2.14812	41.37446	Plaza España 2	13/09/16	28/09/16	29.0	50.2	1141	32.8	1.9	26.5	117052
V25	2.16576	41.38785	Gran Via 589	14/09/16	28/09/16	28.8	50.1	1132	40.8	1.9	33.2	60283
V26	2.16503	41.38763	Balmes 20	14/09/16	28/09/16	28.8	50.1	1132	40.8	1.9	33.2	27093
V27	2.16926	41.39700	Valencia 344	14/09/16	28/09/16	28.8	50.1	1132	40.8	1.9	28	35035
V28	2.15260	41.40631	Torrent de l'Olla 218	09/12/15	22/12/15	57.4	60.5	3653	0	na	21	9916
						BC						
V29	2.15260	41.40631	Torrent de l'Olla 218	17/11/15 13:25	20/11/15 14:30	63.6	83.4	4003	0	1.1	21	9916
V30	2.14857	41.39126	Villaroel 237	26/09/16 9:05	26/09/16 16:45	31.4	66.2	1193	0	na	21	13314
V31	2.21122	41.40634	Ramon Turró 337	28/09/16 8:50	28/09/16 12:45	30.8	79.4	1139	0	na	16.5	2878
V32	2.14812	41.37446	Plaza España 2	21/09/16 8:50	21/09/16 16:00	30.3	57.5	836	0	1.8	26.5	117052

Table 3. List of NO2 and BC vertical profiles and additional relevant parameters. na: not available.

Supplementary material

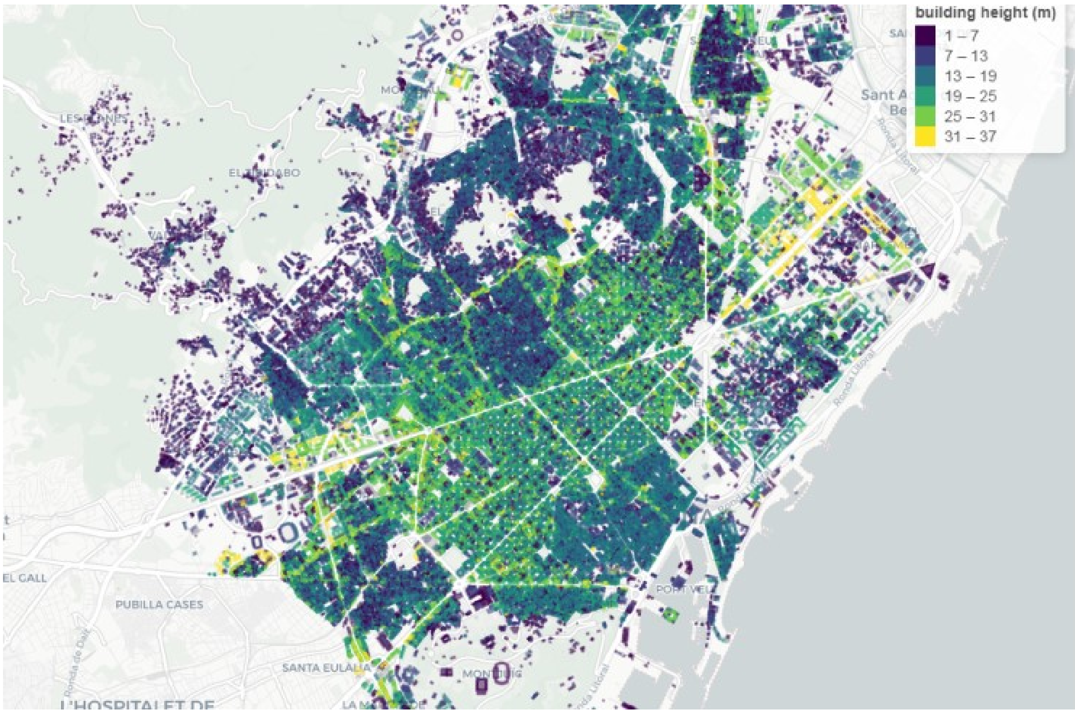

Figure S1. Building height in the city of Barcelona